Glauber-Eikonal Approximation with "Angle" Trajectories: Application to Inelastic (e, H) Scattering

Lars Hambro,*† Joseph C. Y. Chen,† and Takeshi Ishihara‡
Department of Physics and Institute of Pure and Applied Physical Sciences, University of California, San Diego, La Jolla, California 92037
(Received 18 September 1972)

A Glauber-type eikonal approximation with the classical trajectories taken as two intersecting straight-line segments (called "angle" trajectories) is examined and applied to the $2s$ and $2p$ excitation of hydrogen atoms by electron impact. The calculated differential and total excitation cross sections are compared with experimentally measured and "straight-line" Glauber-eikonal cross sections. The angle approximation does provide a significant improvement over the straight-line approximation for the differential cross section at angles $>40°$.

I. INTRODUCTION

Recently, the Glauber-type straight-line eikonal approximation[1,2] has been applied to a number of atomic problems with very encouraging results.[3-6] There are a number of factors which contribute to this success. Formally, it can be shown[7-9] that the Glauber-eikonal approximation contains the second-order multiple scattering terms, in addition to the first-order multiple scattering terms. For atomic problems involving Coulomb pair interactions, the second-order multiple scattering terms remove the singularities of the Coulomb phases in the eikonal approximation.[9] The characteristic Glauber approximation of taking the transverse momentum transfer to be the total momentum transfer (i.e., the longitudinal momentum transfer is neglected) has an intimate influence on the angular dependence of the differential cross section.

It can be shown that the longitudinal momentum transfer has the effect of damping the scattering amplitude [see Eq. (2.19) in Sec. II]. This damping increases with increasing scattering angle. By neglecting the longitudinal momentum transfer, this damping is removed and consequently the scattering amplitude is increased, particularly at large angles.[10] This then partially compensates for the errors introduced by the straight-line approximation. The approximation of taking the transverse momentum transfer [which appears in the argument of Bessel functions, see Eqs. (3.7) and (3.8) in Sec. III] to be the total momentum transfer has the effect of decreasing the inelastic scattering amplitude at small angles, particularly at low energies. Consequently, the Glauber-eikonal approximation yields a total inelastic cross section which is smaller than the other high-energy approximations at the low-energy side. All these features help to yield better results for the Glauber-eikonal approximations.

These characteristic features of the Glauber-type eikonal approximation can be preserved when the classical trajectories are generalized beyond the straight-line trajectories.[9] Chen and Hambro[11] have recently examined the Glauber-eikonal approximation with the classical trajectory approximated by two intersecting straight-line segments (which we call the "angle" trajectory). They have shown that the "angle" trajectory does provide a significant improvement over the straight-line trajectory for both the differential and total elastic scatterings. The purpose of the present paper is to further investigate the Glauber-eikonal approximation for angle trajectories. Calculations are carried out for both the differential and total inelastic (e, H) scatterings.

II. GLAUBER-EIKONAL APPROXIMATION WITH ANGLE TRAJECTORIES

The collision amplitude $\mathcal{J}_{\beta b,\alpha a}$ for a transition $\alpha a \to \beta b$ may be written in terms of the transition operator $T_{\beta\alpha}$ as

$$\mathcal{J}_{\beta b,\alpha a} = \langle \psi_b^{(\beta)} | T_{\beta\alpha} | \psi_a^{(\alpha)} \rangle , \tag{2.1}$$

with

$$T_{\beta\alpha} = \mathcal{U}_\beta + \mathcal{U}_\beta G(E + i\eta)\mathcal{U}_\alpha , \tag{2.2}$$

$$\psi_a^{(\alpha)}(\vec{r}', \vec{R}_\alpha) = \chi_a^{(\alpha)}(\vec{r}')(2\pi)^{-3/2} e^{i\vec{k}_{\alpha a}\cdot\vec{R}_\alpha} , \tag{2.3}$$

$$\psi_b^{(\beta)*}(\vec{r}, \vec{R}_\beta) = \chi_b^{(\beta)*}(\vec{r})(2\pi)^{-3/2} e^{-i\vec{k}_{\beta b}\cdot\vec{R}_\beta} , \tag{2.4}$$

$$E = k_{\beta b}^2/(2\mu_\beta) + \epsilon_b^{(\beta)} = k_{\alpha a}^2/(2\mu_\alpha) + \epsilon_a^{(\alpha)} , \tag{2.5}$$

where $\chi_a^{(\alpha)}(\vec{r}')$ and $\chi_b^{(\beta)}(\vec{r})$ are the products of the asymptotic eigenfunctions with eigenvalues $\epsilon_a^{(\alpha)}$ and $\epsilon_b^{(\beta)}$, respectively; $\mathcal{U}_\alpha$ and $\mathcal{U}_\beta$ are the interaction

potentials in channels α and β, respectively; and $G(E)=(E-H)^{-1}$ is the Green's function of the system. Utilizing the asymptotic channel states given by Eqs. (2.3) and (2.4), we may rewrite Eq. (2.1) in the form

$$\mathcal{J}_{\beta b,\alpha a}=\langle \chi_b^{(\beta)}(\vec{r})|\Upsilon_{\beta\alpha}(\vec{r},\vec{r}')|\,\chi_a^{(\alpha)}(\vec{r}')\rangle\,, \tag{2.6}$$

with

$$\Upsilon_{\beta\alpha}(\vec{r},\vec{r}')=(2\pi)^{-3}\int d\vec{R}_\alpha\, d\vec{R}_\beta\langle \vec{r}\vec{R}_\beta\,|\,T_{\beta\alpha}\,|\,\vec{r}'\vec{R}_\alpha\rangle \times e^{i(\vec{k}_{\alpha a}\cdot\vec{R}_\alpha-\vec{k}_{\beta b}\cdot\vec{R}_\beta)}\,, \tag{2.7}$$

where $\Upsilon_{\beta\alpha}$ is the Fourier transform of the transition operator $T_{\beta\alpha}$ in the coordinate representation.

The well-known Glauber approximation is the straight-line eikonal approximation to Eq. (2.7) for the $\alpha=\beta$ case:

$$\Upsilon_{\alpha\alpha}(\vec{r},\vec{r}')=\delta(\vec{r}-\vec{r}')\frac{ik_{\alpha a}}{\mu_\alpha(2\pi)^3} \times\int d^2b\, e^{i\vec{q}_{ba}\cdot\vec{b}}(e^{i\Phi_\alpha^{(s)}}-1)\,, \tag{2.8}$$

with

$$\Phi_\alpha^{(s)}=\sum_j\Phi_j^{(s)}(b)=\lim_{z\to\infty}\sum_j\left(-(\mu_\alpha/k_{\alpha a})\int_{-\infty}^{z}dz'\,V_j\right), \tag{2.9}$$

$$\mathcal{U}_\alpha\equiv\sum_j V_j\,, \tag{2.10}$$

$$\vec{q}_{ba}=\vec{k}_{\alpha a}-\vec{k}_{\alpha b}=\mu_\alpha(\vec{v}_a-\vec{v}_b)\,, \tag{2.11}$$

where μ_α is the reduced mass in channel α, $\vec{b}=(b,\varphi)$ is a two dimensional vector in the plane perpendicular to the trajectories, $\Phi_j^{(s)}$ are the straight-line eikonal phases due to pair interactions $V_j(\equiv V_{ij})$, and the j sums are over all the pair interactions which constitute the channel potential $\mathcal{U}_\alpha$. We shall consider the application of the eikonal approximation to Eq. (2.7) with $\alpha=\beta$ for the angle trajectory rather than the straight-line trajectory adopted in the Glauber-eikonal approximation.

In the eikonal approximation, we have[2,12,13]

$$\langle \vec{r}\vec{R}_\alpha\,|\,T_{\alpha\alpha}\,|\,\vec{r}'\vec{R}'_\alpha\rangle\, e^{i\vec{k}_{\alpha a}\cdot\vec{R}'_\alpha} \cong\mathcal{U}_\alpha e^{iS^+_{\alpha a}(\vec{R}_\alpha)}\,\delta(\vec{R}_\alpha-\vec{R}'_\alpha)\,\delta(\vec{r}-\vec{r}')\,, \tag{2.12}$$

with the eikonal defined by the path integrals

$$S^+_{\alpha a}(\vec{R}_\alpha)=\int^{\vec{R}_\alpha}(k_{\alpha a}-2\mu_\alpha\mathcal{U}_\alpha)^{1/2}\,ds\,, \tag{2.13}$$

where the path integrals are taken along the classical trajectory with ds denoting the element of path. When the eikonal approximation given by Eq. (2.12) is adopted in Eq. (2.7), we obtain

$$\Upsilon_{\alpha\alpha}(\vec{r},\vec{r}')=\frac{\delta(\vec{r}-\vec{r}')}{(2\pi)^3}\int d\vec{R}_\alpha\,\mathcal{U}_\alpha e^{i(S^+_{\alpha a}-\vec{k}_{\alpha b}\cdot\vec{R}_\alpha)}\,. \tag{2.14}$$

The integral for $\Upsilon_{\alpha\alpha}$ can be evaluated in the cylindrical coordinate system (ρ,z,φ). To relative order $|\theta_c|$ (the classical scattering angle), we have

$$d\vec{R}_a=\rho d\rho dz\,d\varphi\cong b db\,dz\,d\varphi\,. \tag{2.15}$$

The eikonal can be written in the form[13]

$$S^+_{\alpha a}-\vec{k}_{\alpha b}\cdot\vec{R}_\alpha=q_\parallel z+q_\perp b\cos\varphi+\Phi_\alpha(z,b)\,, \tag{2.16}$$

$$q_\parallel=(k_{\alpha a}-k_{\alpha b}\cos\theta)\,,\quad q_\perp=-k_{\alpha b}\sin\theta\,, \tag{2.17}$$

where $q_\parallel$ and $q_\perp$ are the longitudinal and transverse components of the momentum transfer, θ is the scattering angle, and $\Phi_\alpha(z,b)$ are the local eikonal phases which depend also on the internal coordinates of the colliding partners.

When Eqs. (2.15) and (2.16) are utilized in Eq. (2.14), we obtain

$$\Upsilon_{\alpha\alpha}(\vec{r},\vec{r}')=\frac{\delta(\vec{r}-\vec{r}')}{(2\pi)^3}\int d^2b\, e^{iq_\perp b\cos\varphi}\,Q_\alpha(b,\theta)\,, \tag{2.18}$$

with

$$Q_\alpha(b,\theta)=\int_{-\infty}^{\infty}dz\,\mathcal{U}_\alpha e^{i[q_\parallel z+\Phi_\alpha(z,b)]}\,, \tag{2.19}$$

where $Q_\alpha(b,\theta)$ is related to the partial-wave scattering amplitude. The collision amplitude depends sensitively on the accuracy of the eikonal phase. At small scattering angles, the straight-line approximation for the eikonal phase is sufficient. However, at large scattering angles the eikonal phase should be evaluated to a relative order higher than $|\theta_c|$. To evaluate the eikonal phase to relative order θ_c^2, we can make use of a variational principle.[13]

According to the principle of least action,[14] the eikonal is stationary with respect to a variation of trajectory about the exact classical trajectory. If we hold fixed the end points where the system enters and leaves the interaction region, we can determine the trajectory between the two points by minimizing the eikonal. The simplest improvement over the straight-line trajectory is that consisting of two straight-line segments intersecting at an angle 2β. If we consider β to be a variational parameter, and vary β to minimize the eikonal, we would then obtain[13] $2\beta=\theta_c$:

$$\theta_c = \frac{1}{k_\alpha}\frac{d}{db}\Phi_\alpha^{(s)}(b) + O(\theta_c^2),$$

$$= -\frac{b\mu_\alpha}{2k_a^2}\int_{-\infty}^{\infty}\frac{d}{dR_0}\upsilon_\alpha(R_0)\frac{dz}{R_0} + O(\theta_c^2), \qquad (2.20)$$

where $R_0 = (b^2 + z^2)^{1/2}$.

In this case, which we call the "angle" approximation, the eikonal phase takes the form[14]

$$\Phi_\alpha(b) \equiv \lim_{z\to\infty}\Phi_\alpha(z, b) \cong \Phi_\alpha^{(a)}(b), \qquad (2.21)$$

with

$$\Phi_\alpha^{(a)}(b) = \Phi_\alpha^{(s)}(b) + \Delta\Phi_\alpha^{(a)}(b), \qquad (2.22)$$

$$\Delta\Phi_\alpha^{(a)}(b) = (2/v_a)\int_0^{d\sin\beta}\sum_j V_j\, dz, \qquad (2.23)$$

where d is the distance of closest approach of the trajectory to the origin. Comparison of Eq. (2.22) with Eq. (2.9) reveals that the angle approximation differs from the straight-line approximation only by the addition of an extra term in the eikonal phase.

Now, following Glauber by making the approximations

$$q_\perp \approx q_{ba}, \quad q_\parallel \approx 0, \qquad (2.24)$$

the z integral for $Q_\alpha(b, \theta)$ in Eq. (2.19) can be evaluated to relative order $|\theta_c|$

$$Q_\alpha(b, \theta) = i\frac{k_{\alpha a}}{\mu_\alpha}(e^{i\Phi_\alpha^{(a)}} - 1). \qquad (2.25)$$

Notice that Q_α is now no longer θ dependent. This follows from the approximation in dropping the longitudinal momentum transfer $q_\parallel$. As mentioned in Sec. I, this approximation has the effect of increasing Q_α, especially at large angles. Substitution of Q_α from Eq. (2.25) into Eq. (2.18) yields the Glauber-eikonal approximation with angle trajectories, as follows:

$$\Upsilon_{\alpha\alpha}(\vec{r}, \vec{r}') = \delta(\vec{r} - \vec{r}')\frac{ik_{\alpha a}}{\mu_\alpha(2\pi)^3}$$

$$\times\int d^2b\, e^{i\vec{q}_{ba}\cdot\vec{b}}(e^{i\Phi_\alpha^{(a)}} - 1). \qquad (2.26)$$

Thus the simple form of the Glauber-eikonal approximation given by Eq. (2.8) is not altered when the straight-line approximation for the trajectory is generalized to the angle approximation.

III. APPLICATION TO THE (e,H) SCATTERING

As an illustrative example for the application of the Glauber-type eikonal approximation with angle trajectories, we consider the excitation scattering of electrons by hydrogen atoms. The exchange effect will be neglected.

The three-body (e, H) problem involves Coulomb pair interaction. We have for υ_α

$$\upsilon_\alpha = \sum_{j=2}^{3} V_j = \frac{Z_2}{|\vec{R}_\alpha + \gamma_2\vec{r}\,|} + \frac{Z_3}{|\vec{R}_\alpha + \gamma_3\vec{r}\,|}, \qquad (3.1)$$

with

$$\gamma_2 = -(M/m + M), \quad \gamma_3 = (m/m + M),$$
$$Z_2 = 1, \quad Z_3 = -1, \qquad (3.2)$$

where m and M are the masses of the electron and proton, respectively. The straight-line eikonal phase can be readily evaluated from Eq. (2.9). We have

$$\Phi_\alpha^{(s)} = \frac{2\mu_\alpha}{k_{\alpha a}}\ln\left(\frac{|\vec{b} + \gamma_2\vec{s}\,|}{|\vec{b} + \gamma_3\vec{s}\,|}\right), \qquad (3.3)$$

where we have taken the z axis to be parallel to the incident direction and written

$$\vec{r} = \vec{s} + \hat{z}\zeta, \qquad (3.4)$$

with $\vec{s} = (s, \varphi_s)$ denoting a two-dimensional vector in the xy plane. The additional eikonal phase in the angle approximation, given by Eq. (2.23), can be evaluated for Coulomb interaction. We have

$$\Delta\Phi_\alpha^{(a)}(b) \cong 2\frac{\mu_\alpha}{k_{\alpha a}}\, d\sin\beta$$

$$\times\left(\sum_{j=2}^{3}\frac{Z_j}{[|\vec{b} + \gamma_j\vec{s}\,|^2 + (z + \gamma_j\xi)^2]^{1/2}}\right)_{z=d\sin\beta}, \qquad (3.5)$$

where we have made use of Eq. (3.4).

The transition amplitude $\mathcal{J}_{\alpha b,\alpha a}$ given by Eq. (2.6) can now be evaluated using $\Upsilon_{\alpha\alpha}$ obtained from Eqs. (2.26) with eikonal phases given by Eqs. (3.3) and (3.5). The differential cross section is related to the transition amplitude

$$\frac{d\sigma}{d\Omega} = \frac{k_{\alpha b}}{k_{\alpha a}}|(2\pi)^2\mu_\alpha\mathcal{J}_{\alpha b,\alpha a}(\vec{q})|^2. \qquad (3.6)$$

To evaluate $\mathcal{J}_{\alpha b,\alpha a}$, we must evaluate a four-dimensional integral. We have for the $1s \to 2s$ excitation

$$\mathcal{J}_{2s,1s}(\vec{q}) = \frac{i(\sqrt{2})k_{1s}}{4\pi^3\mu_\alpha}\int_0^\infty bdb\,J_0(qb)\int_0^\infty sds\int_0^\pi d\varphi_s\int_0^\infty d\xi\;\Gamma_\alpha[1-\tfrac{1}{2}(s^2+\xi^2)^{1/2}]\;e^{-(3/2)(s^2+\xi^2)^{1/2}}, \tag{3.7}$$

and for the $1s \to 2p_\pm$ excitation

$$\mathcal{J}_{2p_\pm,1s}(\vec{q}) = -\frac{ik_{1s}e^{\pm i\varphi_q}}{8\pi^3\mu_\alpha}\int_0^\infty bdbJ_1(qb)\int_0^\infty s^2ds\int_0^\pi d\varphi_s\cos\varphi_s\int_0^\infty d\xi\;e^{-(3/2)(s^2+\xi^2)^{1/2}}\Gamma_\alpha, \tag{3.8}$$

with

$$q \equiv q_{2s,1s} = q_{2p,1s}, \tag{3.9}$$

$$\Gamma_\alpha = e^{i\Phi_\alpha^{(a)}} - 1 \text{ or } \Gamma_\alpha = e^{i\Phi_\alpha^{(s)}} - 1, \tag{3.10}$$

for angle or straight-line approximations, respectively. $J_0(qb)$ and $J_1(qb)$ are the Bessel functions.

Calculations for the $n=2$ excitation in the (e, H) scatterings are carried out in the Glauber-eikonal approximation. The four-dimensional integrals for the $n=2$ excitation amplitude given by Eqs. (3.7) and (3.8) are evaluated numerically for both the straight-line and angle approximations for the classical trajectories. To account for the rapid oscillation of the integrand, the integration over the impact parameter b is split up into two regions. For $b < 5/q$ Gaussian quadrature is used, and for $b > 5/q$ the integral is evaluated by utilizing the asymptotic expressions of the Bessel functions to recast the integral in the form

$$\sum_j \int_{b_j}^{b_j+\Delta b_j} db_j[g_1(qb)\sin(qb) + g_2(qb)\cos(qb)],$$

where the functions g_1 and g_2 are fairly smooth functions. An explicit evaluation of these integrals is then carried out by fitting the functions g_1 and g_2 into cubic polynomials. The numerical results so obtained in the straight-line approximation are checked against those obtained from the closed expressions derived by Thomas and Gerjuoy.[15] This provides a valuable assessment of the accuracy of the integration routine. The results (numerical error < 8%) are presented and compared with experimental data in graphic form.

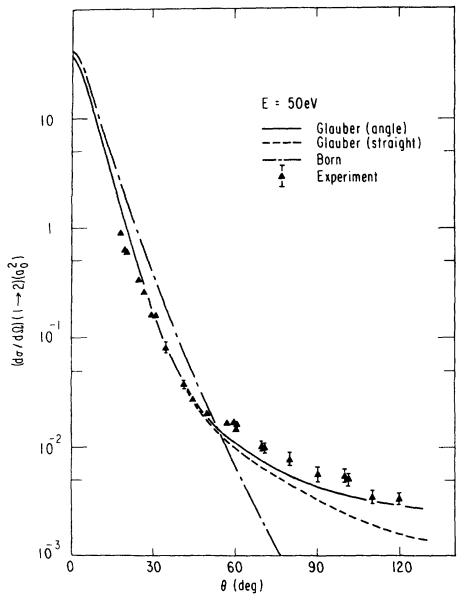

FIG. 1. Comparison of angular dependence of the differential (e, H) $(n = 2)$-excitation cross section at 50 eV in the straight-line and angle Glauber-eikonal approximations and in the first-order Born approximation with experimental data (Ref. 16) which are normalized to the Glauber-eikonal result at an angle of approximately 42°, where the two theoretical curves corresponding to the straight-line and angle approximations come together.

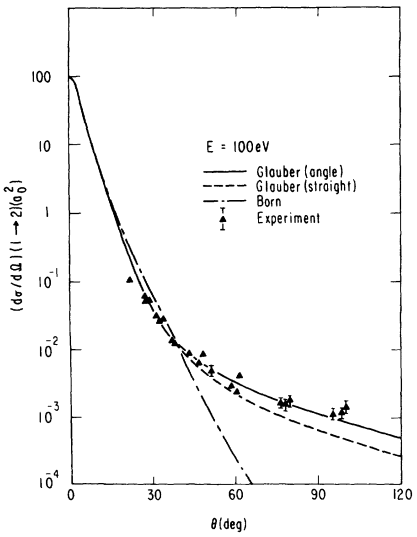

FIG. 2. Comparison of angular dependence of the differential (e, H) $(n = 2)$-excitation cross section at 100 eV in the straight-line and angle Glauber-eikonal approximations and in the first-order Born approximation with experimental data (Ref. 16) which are normalized to the Glauber-eikonal result at an angle of approximately 42°, where the two theoretical curves corresponding to the straight-line and angle approximations come together.

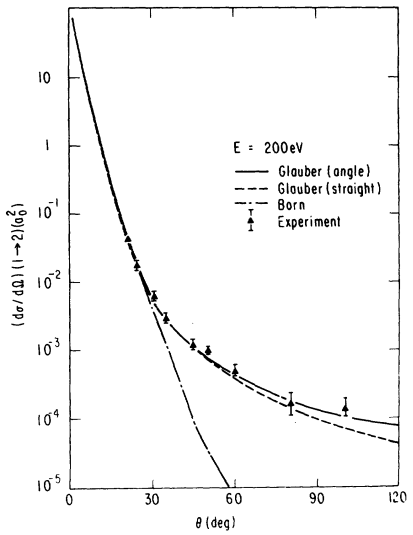

FIG. 3. Comparison of angular dependence of the differential (e, H) $(n = 2)$-excitation cross section at 200 eV in the straight-line and angle Glauber-eikonal approximations and in the first-order Born approximation with experimental data (Ref. 16) which are normalized to the Glauber-eikonal result at an angle of approximately 42° where the two theoretical curves corresponding to the straight-line and angle approximations come together.

IV. RESULTS AND DISCUSSIONS

In Figs. 1–3, the angular dependence of the differential $(n = 2)$-excitation cross section are examined. Figure 1 compares the experimental data[16] with the theoretical angular distributions at an incident electron energy of 50 eV. The experimental data are normalized to the theoretical value at an angle of 42°, where the two theoretical curves corresponding to the straight-line and angle approximations come together. The theoretical results for the $(n = 2)$ excitation are obtained as sums of the $2s$-excitation and $2p$-excitation results. As expected, the angle approximation for the classical trajectories does provide a significant improvement over the straight-line approximation. This is apparent for $\theta > 50°$, where the angle approximation lies between the experimental data and the straight-line approximation. At smaller angles, the difference between the two approximations is too small to be seen for the scale adopted in the figure.

Similar comparisons of the angular dependence of the experimental and theoretical $(n = 2)$-excitation cross sections are given in Figs. 2 and 3 for an incident electron energy of 100 and 200 eV, respectively. The experimental data again are normalized to the theoretical value at an angle about 42°, where the two approximations come together. It is seen that the agreement between the experimental data and the angle approximation is getting better with increasing energies. The deviation between the angle and straight-line approximations also becomes smaller with increasing energies.

For comparison we have included in these figures the result obtained in the first-order Born approximation. At small angles relevant to the determination of the total cross section, the Glauber-eikonal results lie below the Born approximation. The difference between the straight-line and the angle approximation is, however, very small at these angles.

The difference between the two approximations

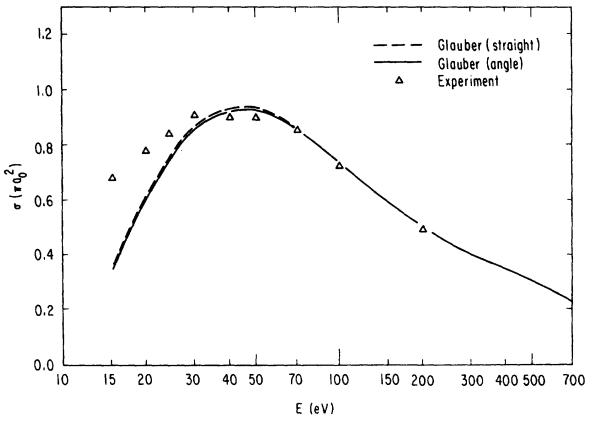

FIG. 4. Comparison of the energy dependence of the total (e, H) $(n = 2)$-excitation cross section in the straight-line and angle Glauber-eikonal approximations with experimental data which are the sum of the data for $2s$ excitation of Kauppila *et al.* (Ref. 17) and the data for $2p$ excitation for Long *et al.* (Ref. 18). Cascade contributions are not included in the theoretical results.

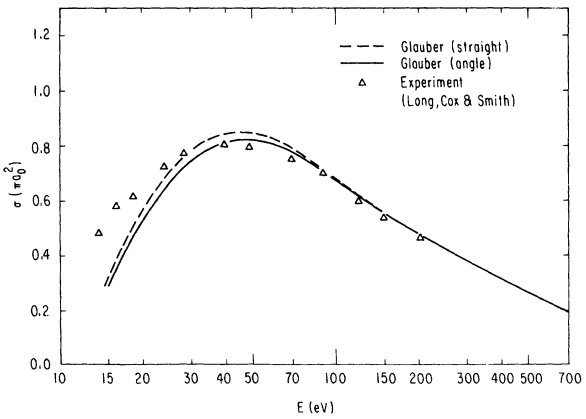

FIG. 5. Comparison of the energy dependence of the total (e, H) $2p$-excitation cross section in the straight line and angle Glauber-eikonal approximations with experimental data of Long *et al.* (Ref. 18).

for the classical trajectories is much more pronounced for the $1s \rightarrow 2s$ excitation than for the $1s \rightarrow 2p$ excitation. This is because the $2p$-excitation amplitude contains significant contributions from large impact parameters. The angle approximation tends to increase the $2s$-excitation cross section but to decrease the $2p$-excitation cross section obtained in the straight-line approximation. As a result, the differential $(n=2)$-excitation cross section (which is the sum of the two excitation cross sections) is decreased at small angles and increased at large angles. The angle approximation therefore yields (Fig. 4) a total $(n=2)$-excitation cross section which is slightly below that given by the straight-line approximation. The experimental data shown in Fig. 4 are obtained by summing over the data for $2s$ excitation of Kauppila *et al.*[17] and the data for $2p$ excitation of Long *et al.*[18] It should be noted that the $2s$-excitation data of Kauppila *et al.* contain significant cascade contributions from higher levels such as the $3p$ state. Thus the shift provided by the angle trajectories is in the correct direction at $E > 40$ eV, although it is small. For $E < 40$ eV, both approximations fail to give the correct shape. This is expected since our approximations are based on the assumption $\theta_c \ll 1$ and $\theta_c \approx 1/E$ for the potential of strength ≈ 1 a.u.

A comparison of the energy dependence of the theoretical and experimental total $2p$-excitation cross section is given in Fig. 5. Here the cascade contribution in the experimental data is small (approximately 2%). The experimental data are those of Long *et al.*[18] computed by Tai *et al.*[4] with the help of the measured polarization of Ott *et al.*[19] It is seen that the angle approximation does provide a better agreement than the straight-line approximation at $E > 40$ eV.

---

*On leave from the University of Oslo, Oslo 3, Norway.

†Research supported in part by the National Science Foundation under Grant No. GP-35738X.

‡Research supported in part by the Atomic Energy Commission under Contract No. AT(04-3)-34, PA 196.

[1]R. Glauber, *Lectures in Theoretical Physics* (Wiley, New York, 1959), Vol. 1, p. 315.

[2]R. L. Sugar and R. Blankenbecler, Phys. Rev. **183,** 1387 (1969).

[3]V. Franco, Phys. Rev. Lett. **20,** 709 (1968); H. Tai, P. J. Teubner, and R. H. Bassel, Phys. Rev. Lett. **22,** 1415 (1969); V. Franco and B. K. Thomas, Phys. Rev. A **4,** 945 (1971).

[4]H. Tai, R. H. Bassel, E. Gerjuoy, and V. Franco, Phys. Rev. A **1,** 1819 (1970).

[5]A. S. Ghosh and N. S. Sil, Indian J. Phys. **44,** 153 (1970), A. S. Ghosh and N. C. Sil, J. Phys. B 4, 836 (1971); K. Bhadra and A. S. Ghosh, Phys. Rev. Lett. **26,** 737 (1971).

[6]F. W. Byron, Jr., Phys. Rev. A **4,** 1907 (1971).

[7]D. R. Harrington, Phys. Rev. **135,** B358 (1964); J. Pumplin, Phys. Rev. **173,** 1651 (1968).

[8]V. S. Bhasin, Nuovo Cimento A **49,** 736 (1967); V. S. Bhasin and V. S. Varma, Phys. Rev. **184,** 1338 (1969).

[9]J. C. Y. Chen, L. Hambro, A. L. Sinfailam, and K. T. Chung, Phys. Rev. A 7, 2003 (1973).

[10]J. C. Y. Chen, R. T. Ling, and T. Ishihara (unpublished).

[11]J. C. Y. Chen and L. Hambro, J. Phys. B **5,** L199 (1972).

[12]D. S. Saxon and L. I. Schiff, Nuovo Cimento **6,** 614 (1957).

[13]J. C. Y. Chen and K. M. Watson, Phys. Rev. 188, 236 (1969).

[14]See, for example, H. Goldstein, *Classical Mechanics* (Addison-Wesley, Reading, Mass., 1950), Chap. 7.

[15]B. K. Thomas and E. Gerjuoy, J. Math. Phys. **12,** 1567 (1971).

[16]K. G. Williams, in *Proceedings of the Sixth International Conference on the Physics of Electronic and Atomic Collisions*, Abstracts of papers (MIT Press, Cambridge, Mass., 1969), p. 731.

[17]W. E. Kauppila, W. R. Ott, and W. L. Fite, Phys. Rev. A **1,** 1099 (1970).

[18]R. L. Long, D. M. Cox, and S. J. Smith, J. Res. Natl. Bur. Stand. (U.S.) A **72,** 521 (1968).

[19]W. R. Ott, W. E. Kauppila, and W. L. Fite, Phys. Rev. A **1,** 1089 (1970).